LEVEL II

12.

OFFICE OF NAVAL RESEARCH

Contract No. N00014-75-C-0922

Task No. NR 056-578

Technical Report No. 14

An Electron Spectroscopic Investigation of the Interaction of Methanol with Polycrystalline Aluminum

by

J.W. Rogers, Jr., R.L. Hance and J.M. White

Prepared for Publication

in

Surface Science

Department of Chemistry

University of Texas at Austin

Austin, Texas 78712

June 15, 1980

DISCLAIMER NOTICE

THIS DOCUMENT IS BEST QUALITY PRACTICABLE. THE COPY FURNISHED TO DTIC CONTAINED A SIGNIFICANT NUMBER OF PAGES WHICH DO NOT REPRODUCE LEGIBLY.

SECURITY CLASSIFICATION OF THIS PAGE (When Date Entered)

REPORT DOCUMENTATION PAGE

READ INSTRUCTIONS BEFORE COMPLETING FORM

1. REPORT NUMBER

2. GOVT ACCESSION NO. AD-A087309

3. RECIPIENT'S CATALOG NUMBER (9)

4. TITLE (and Subtitle)

(6) An Electron Spectroscopic Investigation of the Interaction of Methanol with Polycrystalline Aluminum.

5. TYPE OF REPORT & PERIOD COVERED
Technical Report
~~1 January, 1980 - 31 Dec. 1980~~

6. PERFORMING ORG. REPORT NUMBER
1 Jan - 21 Dec 80

7. AUTHOR(s)

(10) J. W. Rogers, Jr., R.L. Hance and J.M. White

8. CONTRACT OR GRANT NUMBER(s)
(15) N00014-75-C-0922

9. PERFORMING ORGANIZATION NAME AND ADDRESS
J.M. White, Department of Chemistry
University of Texas at Austin
Austin, Texas 78712

10. PROGRAM ELEMENT, PROJECT, TASK AREA & WORK UNIT NUMBERS
Project NR 056-578

11. CONTROLLING OFFICE NAME AND ADDRESS
Department of the Navy
Office of Naval Research
Arlington, Virginia 22217
(11) 15

12. REPORT DATE
June 1980

13. NUMBER OF PAGES
34

14. MONITORING AGENCY NAME & ADDRESS(if different from Controlling Office)
(12) 20

15. SECURITY CLASS. (of this report)

15a. DECLASSIFICATION/DOWNGRADING SCHEDULE

16. DISTRIBUTION STATEMENT (of this Report)

Approved for Public Release; Distribution Unlimited
(14) TR-14

17. DISTRIBUTION STATEMENT (of the abstract entered in Block 20, if different from Report)

18. SUPPLEMENTARY NOTES

Preprint, accepted, Surface Science

19. KEY WORDS (Continue on reverse side if necessary and identify by block number)

20. ABSTRACT (Continue on reverse side if necessary and identify by block number)

X-ray and ultraviolet photoelectron spectroscopic results are reported for the interaction of CH_3OH with clean polycrystalline Al in the temperature range 110-500 K. Methanol is molecularly chemisorbed at low exposure and low temperature (110 K) followed by condensation at higher exposure. The multilayers desorb beginning near 170 K and the chemisorbed layer is converted into a surface methoxide. Room temperature adsorption also leads to formation of the methoxide species which is stable to ~500 K, at which point it decomposes evolving CH_4 and leaves the surface oxidized.

DD FORM 1 JAN 73 1473 EDITION OF 1 NOV 65 IS OBSOLETE
S/N 0102-014-6601

SECURITY CLASSIFICATION OF THIS PAGE (When Date Entered)

347830 APPROXIMATELY

Surface Sci.
(in press)
5-80

An Electron Spectroscopic Investigation of the Interaction of Methanol with Polycrystalline Aluminum.[a]

J.W. Rogers, Jr.,[b] R.L. Hance,[c] J.M. White

Department of Chemistry
University of Texas
Austin, Texas 78712

Abstract

X-ray and ultraviolet photoelectron spectroscopic results are reported for the interaction of CH_3OH with clean polycrystalline Al in the temperature range 110-500 K. Methanol is molecularly chemisorbed at low exposure and low temperature (110 K) followed by condensation at higher exposure. Bonding mechanisms and geometries in the condensed and chemisorbed layers are discussed. The multilayers desorb beginning near 170 K and the chemisorbed layer is converted into a surface methoxide. Room temperature adsorption also leads to formation of the methoxide species which is stable to ~500 K, at which point it decomposes evolving CH_4 and leaves the surface oxidized.

(a) Supported in part by the Office of Naval Research.

(b) Present Address: Division 2516, Sandia Laboratories, Albuquerque, New Mexico 87185.

(c) Visiting Professor, Permanent Address: Department of Chemistry, Abilene Christian University, Abilene, Texas 79601.

1.0. Introduction

Being the building block for many important synthetic reactions as well as having an increasingly important role in the growing energy crisis, the production of CH_3OH is increasing annually[1]. The fact that CH_3OH can be mixed with gasoline to improve engine performance [2], used as a feedstock to produce gasoline [3], used alone as a fuel [4], or used as a hydrogen carrier in fuel cell technology illustrates its importance. Its reactions and behavior on various catalysts and in a variety of environments is clearly important.

On a fundamental level CH_3OH is structurally simple, well understood theoretically [6], and, being its smallest member, represents a broad class of organic compounds, the alcohols. In addition its gas phase UPS and XPS spectra are well understood which, coupled with its high vapor pressure at room temperature, makes it attractive for adsorbate studies on various substrates. As such it has been studied on single crystal Ni [7,8], W [9,10], Ru [11], and Cu [12], as well as polycrystalline Pd [13]. Its interaction on MoS_2 [14], oxidized Cu [12], and both single crystal and polycrystalline ZnO [15,16] have also been reported.

On transition metals, condensation occurs at low temperature (~80-100 K) and a methoxide complex has been identified in the 150-180 K temperature range. At room temperature CH_3OH decomposes to CO and hydrogen on these metals. The present study was prompted by our interest in the study of chemisorption on non-transition metals and their oxides. A preliminary report on this investigation has been presented elsewhere [17]; in this paper we report both UPS and XPS data for the adsorption and decomposition of CH_3OH on Al over the temperature range 110-500 K.

2.0. Experimental

The data were taken on a PHI Model 548 electron spectrometer using pulse counting techniques and stored on a digital signal averager. A 20 eV window was typically scanned 16 times at a rate of 1.56 eV/sec. This gave typical count rates of 200 cps in XPS and 50 cps in the He II UPS. Binding energies were referenced to the Fermi level of Al; in this manner the measured Al(2$\mathscr{p}$) BE was 117.6 eV. The CMA was operated in the retarding mode at a constant resolution of 0.4 eV (FWHM) for He II and 1.6 eV for XPS. The photoelectric work function was measured from the width of the kinetic energy distribution by applying a small negative bias (3-6 volts) to accurately determine the onset of secondary emission. The XPS data were taken with a Mg Kα source and the UPS data with a differentially pumped He-discharge source.

The sample consisted of ~1 cm^2 of 99.999% Al foil which was clamped to a button heater assembly. The latter could be cooled to 106 K and heated to 700 K and its temperature was monitored with an attached chromel-alumel thermocouple.

Methanol was admitted to the sample through a carefully calibrated [18] multi-channel array doser from a dynamically pumped ballast. The doser was situated less than 0.5 cm from the sample. By this method a one Langmuir (1L = 10^{-6} torr-sec) CH_3OH exposure could be obtained in 150 sec while eliminating flux gradients across the surface and without raising the total system pressure above 9×10^{-10} torr.

The Al sample was cleaned at room temperature by Ar^+ ion bombardment at 5KV (8 milliwatt/cm^2). The initial cleaning took about 11 h while subsequent cleanings, after exposure to CH_3OH, required 0.5 h. The sample was not annealed after sputtering.

3.0. Results

3.1. Low Temperature Adsorption of CH_3OH

The XPS spectral features of both substrate and adsorbate transitions clearly indicate that, below 130 K, CH_3OH is nondissociatively adsorbed at low exposures and is condensed at high exposures. These results are presented in the ensuing paragraphs with further confirmation coming from the UPS results presented in Sec. 3.2.

3.1.1. Changes in XPS Spectral Features as a Function of Exposure

The O(1s) and C(1$\mathscr{s}$) regions as a function of CH_3OH exposure at 110 K are shown in Fig. 1. With increasing CH_3OH exposure the O(1s) transition increases in intensity and BE while its peak width decreases at higher exposures as seen in spectra a-c. Similar behavior is noted for the C(1s) transition in curves d-f. The extent of CH_3OH decomposition can be determined by comparing O(1s) and C(1s) relative peak areas. After correcting the area of curve b for analyzer transmission and scaling its area by the C(1s)/O(1s) sensitivity ratio, a C(1s) peak area within 4% of that of c is obtained. This indicates that very little, if any, CH_3OH is decomposed to form Al_2O_3 in contrast to the interaction of D_2O with Al [19,20] where extensive decomposition occurs. This conclusion is supported by measurements on the Al(2s) BE and the UPS spectra of adsorbed species as discussed below. In view of this, the BE's of 532.2 and 286.7 eV for the O(1s) and C(1s) respectively are assigned to molecular CH_3OH. The BE's from Fig. 1 are summarized in Table 1.

A small amount of oxygen (not shown) remains after sputter cleaning; it is comprised of surface and subsurface oxygen and is equivalent to less than 5% of a surface monolayer. Its BE is near 531.5 eV which is close to that of bulk Al_2O_3 (531.3 eV).

The O(1s) relative peak area versus CH_3OH exposure (~120 K) is plotted in Fig. 2. There is a monotonic increase to a limiting value at 150 L. At this low temperature, multilayer formation occurs and the limiting value of the O(1s) peak area is reached when the thickness of condensed CH_3OH becomes greater than the analysis depth of ~50 Å (determined by the electron kinetic energy).

The exposure at which multilayer formation begins cannot be determined from the figure, but can be estimated from the attenuation of the substrate-derived Al(2s) intensity as follows. Fig. 3a displays the Al(2s) relative intensity as a function of CH_3OH coverage (from Fig. 2). As expected, the Al(2s) intensity is attenuated as the CH_3OH coverage increases. Assuming a uniform overlayer, the multilayer thickness, in Å, can be approximated from

$$I = I_o \exp(-d/\lambda) \qquad (1)$$

where I and I_o are the intensity of adsorbate covered and clean Al, d is the multilayer depth and λ is the Al(2s) attenuation length (17 Å [18,21]). Further assuming CH_3OH to be a hard sphere of diameter 4.5 Å [22], the number of molecular layers at several coverages can be calculated and are indicated on the figure. Noteworthy is the completion of one monolayer at a relative coverage of 0.34. This is important in the discussion of the behavior of peak widths and BE's presented below.

The BE of the C(1s) and O(1s) transitions as a function of relative CH_3OH coverage is shown in Fig. 3b. Both increase with coverage until the first monolayer ($\theta \approx 0.4$) is completed. With further adsorption there is a region of constant BE to $\theta \approx 0.7$ after which increases are noted to limiting values of 534.5 and 288.3 eV for the O(1s) and C(1s) transitions respectively.

Notice that O(1s) BE's are shown at low exposure with no corresponding C(1s) BE. This is due to (1) the existence of some residual oxide-like O(1s) signal after cleaning that is attributable to sub-surface oxygen as previously mentioned, and (2) the higher relative sensitivity for oxygen as compared to carbon, makes the former detectable at lower concentration than the latter. The presence of O(1s) intensity and the absence of corresponding C(1s) intensity at low exposure is therefore not an indication of CH_3OH dissociation.

The general behavior of the 1s BE's shown in Fig 3b, in conjunction with the multilayer depths as a function of coverage from Fig. 3a, suggests the following interpretation. The BE's for sub-monolayer coverages of molecularly adsorbed CH_3OH are 532.3 ± .3 and 286.7 ± .3 eV for O(1s) and C(1s) respectively. As condensation begins, the BE's of both levels shift to higher values (533.3 and 287.2 eV respectively) characteristic of the multilayer and remain constant to a coverage near 0.7 (~4 molecular layers). Further exposure produces a condensed layer which is thick enough to insure that no metal derived relaxation effects occur in the final state. The BE's thus increase to limiting values of 534.4 and 288.3 eV at exposures of 150 L (the highest exposure of the present study). Surface charging in the condensed layer was not a problem at these coverages as tested with two methods suggested by Briggs [21].

These results show that the O and C 1s levels are relaxed by at least 2.1 and 1.6 eV respectively as calculated from BE differences at relative coverages of 1.0 and 0.2. These final state effects are due to extra-atomic relaxation. The actual extra-atomic relaxation energy is defined as the BE difference between equivalent levels in chemisorbed and gas phase CH_3OH. For CH_3OH/ these values are 3.7 and 2.7 eV for the O and C 1s levels respectively. The core hole size and the kinetic energies of the O(1s) and C(1s) photoelectrons

can account for part of the difference in relaxation energy between these two levels, but not a difference as large as 1 eV. If the oxygen end of the molecule is bonded to the surface, electrostatics involving the distance of the carbon and oxygen atom from the image plane of the surface can account for the additional shift [24]. A good discussion of the effect of distance from the surface on core level binding energies has been given by Fisher et al. [24a] for the case of SF_6 physisorbed on Ru(001).

Even more interesting is the spacing between the O and C 1s levels in the adsorbed phase. It is consistently 0.5 eV less than the gas phase spacing even at low exposure. The origin of such a large differential shift in energy levels between the gas and condensed phases may be due in part to substrate-related relaxation effects in the adsorbed layer. It is tempting to ascribe the remainder of the shift to perturbations of the oxygen core levels arising from hydrogen bond formation in the condensed layer. The UPS results discussed below confirm that hydrogen bonding shifts the valence orbital energies.

We have previously shown that condensation enhances the surface sensitivity of substrate-derived XPS electrons by increasing the bulk-to-surface attenuation ratio [18]. Formation of an oxide layer on Al, the depth of which is less than the mean free path of the Al(2s) electron, followed by multilayer adsorption of a condensible gas, leads to a shift to higher BE of the Al(2s) transition. As D_2O condenses on clean Al such a shift is observed indicating that the D_2O is dissociated and the Al substrate oxidized prior to the onset of condensation [19]. The absence of a similar shift in the present case is further evidence that CH_3OH is not dissociated prior to condensation.

The behavior of the C and O 1s peak widths (FWHM) with increasing CH_3OH exposure is shown in Fig. 3c. At low coverage, the widths of the transitions

are ~3.2 eV. As coverage increases the widths of both peaks steadily decrease to limiting values of ~2.1 and 2.3 eV for the C and O transitions respectively. The 1s peak widths are expected to be larger at sub-monolayer coverage than at high coverage due to the variety of heterogeneous adsorption sites on the metal surface and, in the case of the O(1s) transition, due to the superposition of CH_3OH and residual oxide-like intensity (which remains after sputtering). After completion of the first monolayer the peak width should steadily decrease with further exposure to a limiting value characteristic of condensed CH_3OH. The limit will be reached when the multilayer depth achieves proportions at least as large as the analysis depth. This is consistent with the observed behavior. The C(1s) widths are smaller at each coverage than the corresponding O(1s) widths; ~0.1 eV of this is due to differences in the core hole lifetimes of C and O [25].

At an exposure of 150 L, shown in c and f of Fig. 1, CH_3OH has condensed on the surface and the peak widths are 2.3 and 2.1 eV for the O(1s) and C(1s) transitions. The O(1s) peak width is identical to that reported by Siegbahn, et al. for condensed CH_3OH [26].

3.1.2. UPS Results: Mechanism of CH_3OH Bonding at Low Temperatures

While XPS spectral features are useful in measuring relative concentrations of adsorbed species and are sensitive to the local chemical environment, particulars of the bonding mechanism require a probe of the valence levels of both the adsorbate and the underlying substrate. In the present case, the UPS spectral features are particularly revealing.

The gas phase UPS ($\hbar\omega$ = 21.2 eV) spectrum [27] of CH_3OH is shown in Fig. 4, along with representations of the orbitals from which the transitions arise [28]. The four bands were assigned by Eland [29] and later clarified

by molecular orbital calculat'ons [6,30]. The first band, labelled 2a", arises through the ionizat on of electrons in an out-of-plane, non-bonding orbital on oxygen. A companion orbital, which would be degenerate with the 2a" were the C-O-H linkage linear, is the 7a' which determines, in part, the H-O-C bond angle. Another pair of orbitals, 1a" and 5a', would also be degenerate were H-O-C linear. These orbitals are largely associated with the methyl group, but the latter involves the C-O-H region as well. The 6a' orbital is a σ-bonding H-O-C-H orbital. Another ionization, not shown in Fig. 4, is accessible with He II radiation. It is labelled 4a' and involves a weakly-bonding core-like C(2s) orbital.

The UPS spectra for the adsorption and condensation of CH_3OH on clean Al at 110-300 K have been reported previously in a preliminary publication [17]. These spectra, shown in Fig. 5, have been partially reinterpreted in light of the XPS results. The BE's are summarized in Table 1. Difference spectra are not necessary for our purposes due to the essentially flat nature of the Al valence band shown in 5a. Argon-ion sputtered Al exhibits a broad low intensity peak centered near 7 eV. This is due to the O(2p) resonance from a small quantity of oxygen which remained after cleaning. The work function of polycrystalline Al, measured from the width of the kinetic energy distribution, is 4.2 eV. This agrees well with the average value of the work function for different faces of Al single crystals [31].

Spectra (d) and (e) in Fig. 5 are for CH_3OH adsorption at 110 K and correspond to one monolayer ($\Delta\Phi$ = -1.0 eV) and multilayer ($\Delta\Phi$ = -1.3 eV) respectively. We have used the monolayer coverage spectrum (d) as a reference and have shifted spectrum (e) 0.6 eV to

lower binding energy to align the $(\widetilde{1a''})^{-1}$ transitions (BE = 11.0 eV). This facilitates comparison of energies and compensates for the loss of final state screening in the condensed multilayer. This alignment was chosen for the following reason [37]. There exists evidence that alcohols, aldehydes and ketones all bond to metals end-on through the oxygen atom [36]. Assuming this to be the case for the CH_3OH/Al system of the valence orbitals, one would expect the $(\widetilde{1a''})^{-1}$ transition to be least likely to participate in a surface bond because it is not geometrically oriented to do so. The $(\widetilde{6a'})^{-1}$ transition would also tend to be unaffected because of its σ-character would the $(\widetilde{5a'})^{-1}$ transition due to its methyl character. Curve e shows the five well resolved peaks, situated between 6 and 19 eV, which are expected in this energy range from gas phase UPS studies on CH_3OH. Parenthetically we note that in Fig. 5e, the two low intensity peaks at ~1.5 eV above and ~3 eV below E_F are due to excitation of the $\widehat{2a''}$ and $\widehat{1a''}$ - $\widehat{6a'}$ orbitals of condensed CH_3OH by He II ($3s \rightarrow 1s$) photons ($h\nu$ = 48.31 eV).

The experimental gas phase vertical ionization energies, ϵ_i, from Robin and Kuebler [6] are also displayed in the figure after referencing these levels to the Fermi level of spectrum e.

This has been done using the constant local work function method described by Hagstrom [37]. The referencing is achieved by subtracting from the gas phase IP's both the work function of clean aluminum and the change in work function which is measured for a methanol saturated surface [BE (E_F=0) = ($\epsilon_i - \Phi_{Al} - \Delta\Phi_{sat}$)]. The value of $\Delta\Phi_{sat}$ = -1.3 volts was used

For chemisorbed layers, extra-atomic relaxation/polarization energy for valence levels is defined by $E^R = [BE^{gas}\ (E_F = 0) - BE^{ads}\ (E_F = 0)]$ for an orbital which is known not to participate in surface bond formation. As mentioned above, we consider that the $\widetilde{1a}$" orbital most nearly fulfills this criterion. We have chosen this orbital for estimating the extra-atomic relaxation polarization energy even in the multilayer spectra and, on this basis, the valence orbital relaxation energy in the multilayer is 0.9 ± 0.1 eV (See Table I and remember that the condensed phase spectrum has been shifted 0.6 eV to align it with the chemisorbed spectrum). Within experimental error, the $\widehat{6a}'$, $\widehat{5a}'$ and $\widehat{2a}$" orbitals are relaxed by the same amount while the $\widehat{7a}'$ and $\widehat{3a}'$ show an additional shift of 0.4 eV to higher BE. We do not understand the differential shift of the $\widehat{4a}'$ ionization and only note that similar differential shifts of analogous C(2s) orbitals have been observed where rehybridization occurs during chemisorption [38]. In the present multilayer case, strong hydrogen bonding may give some electronic rearrangement at the carbon. The shift of the $\widehat{7a}'$ is interpreted as an initial state effect due to hydrogen bonding in the condensed multilayer.

There is some support for this point of view in the analogous UPS spectral features of ice [39] where the $3a_1$ orbital was shifted further from its gas phase value than the $1b_2$ orbital. This differential shift is attributable to hydrogen bonding. The corresponding orbitals in methanol are the 7a' and the 6a' respectively. Since the hydrogen bond strengths are similar (6.2 and 4.5 kcal mole^{-1} for CH_3OH and H_2O [40]), we expect similar differential shifts. This comparison cannot be pushed too far since H_2O forms a tetrahedral crystal while CH_3OH does not.

(SL)
Chemisorption of CH_3OH at 110 K is shown in curve d. The relative intensities of the $\widetilde{7a}'$ and $\widetilde{5a}'$ orbitals have increased with respect to the $\widetilde{6a}'/\widetilde{1a}$" orbitals as compared to the condensed phase. The large decrease in intensity and apparent broadening of the 2a" peak as well as a slight shift (~0.1 eV) to higher BE is evidence that bonding to the Al is occurring through the lone-pair electrons on oxygen as has been the case in general for alcohol-type molecules on metals [36]. Vibrational broadening of this level is indicative of a strong bonding interaction with the surface. The negative work function change, $\Delta\Phi = -1.0$ eV, accompanying chemisorption of CH_3OH during a 5 L exposure supports the conclusion that the oxygen end of the molecule bonds to the surface. The existence of four peaks in the valence region suggests that this species is molecularly chemisorbed without cleavage of the hydroxyl hydrogen.

The constant local work function method can also be applied to the saturated chemisorbed methanol system to determine an orbital relaxation energy. The work function change for this saturation case is $\Delta\Phi = -1.0$ eV and, with respect to the gas phase, the relaxation energy is 1.2 ± 0.1 eV as compared to 0.9 eV in the saturated multilayer case. Comparing spectra 5d and 5e, indicates a major differential shift of the 7a' orbital (0.6 eV) and a smaller shift of the $\widehat{4a}'$ orbital (0.3 eV). There is no measurable differential shift in the other ionizations. Since the $\widehat{7a}'$ orbital is heavily involved in establishing the C-O-H angle a steric distortion in this region due to the close proximity of the O-H and lone pair-surface bonds could cause such a differential shift. Both calculation and experiment have shown shifts of similar magnitude in the CH_3OH/Ni (111) system [30].

Compared to the gas phase and referenced to the $\widetilde{1}a''/\widetilde{6}a'$ pair, the $\widetilde{2}a''$, $\widetilde{4}a'$ and $\widetilde{5}a'$ orbitals are differentially shifted to lower BE by a small amount (~0.15 eV) while the $\widetilde{7}a'$ is differentially shifted to higher values by about the same amount. This can be interpreted reasonably in terms of a molecularly adsorbed methanol species perturbed slightly from its gas phase geometry, but perturbed in a way that is distinguishable from multilayer methanol.

Robin and Kuebler [6] have shown that the 2a" and 7a' orbitals would be degenerate if CH_3OH were a cylindrical molecule with a linear C-O-H portion where H is the hydroxyl hydrogen. Thus, a steric distortion that tends to increase the C-O-H angle should shift the BE's of the $\widetilde{2}a''$ and $\widetilde{7}a'$ orbitals closer together. However, the $\widetilde{5}a'$ and $\widetilde{1}a''$ orbital energies are also degenerate and should shift toward a common BE under these conditions. From the BE's listed in Table 1, this doesn't appear to be the case, but it should be remembered that the $(1a'')^{-1}$ and $(6a')^{-1}$ transitions are badly overlapped and such a shift could be manifested in a broadening of the $(\widetilde{1}a'')^{-1}/(\widetilde{6}a')^{-1}$ band rather than a shift in the $\widetilde{5}a'$ BE with respect to the peak maximum. This may very well be the case, but it is difficult to tell from Fig. 5.

3.2. Adsorption at Higher Temperatures and the Thermal Stability of Adsorbed CH_3OH and Methoxide

3.2.1. Low Temperature Adsorption of CH_3OH Plus Heat

Figure 6 shows the behavior of the O, C and Al core-level relative peak areas for a condensed multilayer of CH_3OH as the surface temperature is slowly increased. Initially, the Al substrate was exposed to 30 ℓ of CH_3OH at 120 K. The surface temperature was then raised to the indicated temperatures by termination of the liquid nitrogen flow and immediately recooled for spectroscopic analysis. The Al(2s) peak areas were normalized to the value for clean Al while the C and O (1s) areas were normalized to the values measured for the initially condensed multilayer.

Beginning at ~160 K, the C and O areas decrease rapidly to a constant value of ~0.3. The O(1s)/Al(2s) integrated peak area ratios at 260 K are within 17% of those for a saturated room temperature adsorption of CH_3OH, indicating that ~1 monolayer of a chemisorbed, CH_3OH-derived moiety remains on the surface after desorption of the condensed multilayer. Concurrent with the decrease in the oxygen and carbon signals is an increase in the Al(2s) signal as the multilayers desorb. The Al peak area at 260 K is also comparable to that obtained from saturation CH_3OH coverage at room temperature. The overlayer depth at this temperature, as estimated from the Al(2s) relative peak area is 3.7 Å, and assuming a CH_3OH diameter of roughly 4.5Å, this is in good agreement with a monolayer of chemisorbed species remaining after desorption of the multilayer.

Independent thermal desorption measurements (TDS) at a heating rate of 13 K/sec. show that CH_3OH is molecularly desorbed, the desorption temperature maximum being T_{des} = 187 K. Assuming first-order desorption and pre-exponential factor of 10^{13} $sec.^{-1}$, this corresponds to an activation energy of desorption of E_{des} = 10.8 kcal/mole [41]. This value is within 4% of that

calculated from the reported desorption temperatures for CH_3OH condensed on Ni(100) [42] and is within 16% of the heat of vaporization of CH_3OH reported by Edwards [43] who used a more appropriate zeroth-order rate law for the desorption kinetics.

The work function change accompanying condensation of CH_3OH is -1.3 eV. After multilayer desorption $\Delta\Phi$ moves from -1.3 to -0.9 eV. The direction and magnitude of the work function change (compared to the work function of clean Al) indicate that a species with a substantial dipole moment, the negative end facing the surface, remains at 260 K. Some characteristics of this surface species can be determined from changes in UPS spectral features with temperature and from room temperature adsorption of CH_3OH.

3.2.2. High Temperature Adsorption of CH_3OH

The UPS ($h\nu$ = 40.8 eV) region for the adsorption of CH_3OH on clean Al at 300 K is shown in curves b and c of Fig. 5. They are significantly different from those at low temperature (d and e) in two respects: (1) only three peaks are clearly resolved instead of five, and (2) the two main peaks in the valence band are broader than their counterparts at low temperatures. A shoulder on the low BE side of the two peaks at 6.8 and 10.6 eV is also present. The species giving rise to these spectra were also found by Rubloff on Ni(111) in the temperature range of 160-300 K [30,44]. It is clear that curve b derives from a chemisorbed species because the Fermi level has not been attenuated. The close resemblance of its three main features with features in curves d and e indicates that a species with similar structure is responsible for these spectra. Curves b and c are assigned as methoxide, i.e., the O-H bond of the hydroxyl group has been cleaved, for reasons outlined in the following paragraphs.

Assuming methoxide, one would expect the $\tilde{1}a''$ to be least affected since it is localized on the methyl group which does not participate directly in the surface bond formation. All the other orbitals shown in Fig. 5 would be expected to shift since they all involve the OH region of CH_3OH. Comparing 5b and 5c to 5d and 5e indicates that the $\tilde{7}a'/\tilde{2}a''$ and the $\tilde{5}a'/\tilde{1}a''$ orbitals have shifted towards one another and are no longer resolvable. The O-bonding $\tilde{6}a'$ orbital does not appear to be split off from the $\tilde{5}a'/\tilde{1}a''$ region, but the data allow very little to be said about this point.

As noted above, a linear C-O-H portion of CH_3OH would make the 5a' and 1a" orbitals and the 7a' and 2a" orbitals degenerate. From the observed shifts it can be concluded that the methoxide species has a C-O-Al portion which has a bond angle closer to 180° than the analogous C-O-H portion of adsorbed or gaseous CH_3OH. Since the two peaks near 7 and 11 eV in c have widths ~4 eV, it is apparent that each peak is the superposition of two closely spaced transitions indicating that the methoxide is not completely linear (C-O-Al angle ≠ 180°). This is in agreement with LELS results for methoxide on Ni where it was shown that the C-O-Ni angle is oblique [8]. It is not unreasonable to expect a surface methoxide since Al/methoxide complexes constitute a well known, stable class of compounds in inorganic chemistry; transition metal/methoxide complexes are known to exist for Ni, W and Zn (among others) but have not been extensively studied [45,46].

One must consider other oxygen containing intermediates which might produce the spectra shown in Fig. 5. When the gas phase IP's of formic acid, formaldehyde and CO are referenced to the Fermi level of Al, and superimposed over the spectra in the figure, the agreement with the observed peaks is poor suggesting that these species are not formed.

The XPS and thermal desorption results provide further evidence for methoxide formation above 190 K. The C and O(1s) regions are shown in Fig. 7

for CH_3OH and O_2 adsorption at various temperatures. Curves a and b result from the adsorption of CH_3OH at 300 and 110 K respectively. The BE of the O(1s) transition is lower in the latter case. Adsorption of O_2 at 110-300 K (curve c) gives rise to an oxygen transition at even lower BE. The C(1s) results for room temperature and low temperature CH_3OH adsorption (d and e) show similar behavior. Curve f shows the effect of adsorbing CH_3OH at 110 K followed by increasing the surface temperature to 300 K. The peaks in d and f have identical BE's and similar results are obtained for the O(1s) transition.

The electron BE's for the various species are summarized in Table 1. The coordination around the oxygen atom would be greater in chemisorbed CH_3OH than for a surface methoxide; consequently, the local electron density could be higher and the BE lower for the former. This is reflected in the experimental results in that both the carbon and oxygen core levels are shifted 0.4 eV during the transformation from chemisorbed CH_3OH to methoxide. This perturbation of the core levels would be expected if the valence molecular orbitals with significant carbon and oxygen character ($6a'$ and $5a'$) are chemically shifted toward a common BE as in the present case.

The results of thermal desorption measurements show that the methoxy-surface complex decomposes at ~500 K, evolving CH_4 and leaving some carbon that is detected by AES. Assuming a value of 10^{13} $sec.^{-1}$ for the pre-exponential factor of a surface enhanced decomposition [47], and assuming the decomposition to be first-order [41], the activation energy for the rate limiting step of the decomposition is 29.9 kcal/mole. No CO, H_2O, or CH_3OH was desorbed above room temperature.

CH_4 is an unlikely gas phase product without the presence of surface methoxide. Aluminum methoxide (liquid phase) decomposes to CH_4, H_2, CO and CH_3OCH_3 in the temperature range 573-653 K [46]. There is no evidence for desorption of CH_4 following adsorption of CH_3OH at 300 K on Ni, Ru, or W [30,11,10].

Fig. 8 shows the UPS results of the decomposition of the methoxide complex. Curve a is obtained by chemisorbing 27 L of CH_3OH at room temperature. Heating the surface to 573 K converts a into b. Curve b is identical in width, shape, and BE with the O(2p) resonance obtained from oxidation of Al with O_2 at 110-673 K. The O(1s) BE for the species in curve a is 532.7 eV; this shifts to 531.3 upon heating which confirms the conversion to bulk oxide beginning at ~500 K. The O(1s) peak area before and after desorption shows that more than 93 ± 5% of the oxygen contained in the methoxide species remains on the surface after desorption.

4.0. Conclusions

XPS, UPS and TDS techniques have been used to characterize the interaction and thermal stability of CH_3OH on clean Al surfaces. CH_3OH molecularly chemisorbs at temperatures less than 130 K. The magnitude of the work function change, structure of the CH_3OH valence region, and comparison of the C and O(1s) BE's all indicate that CH_3OH is chemisorbed, the surface bond being formed through the oxygen orbitals, without cleavage of the hydroxyl hydrogen. Further exposure leads to condensation where strong hydrogen bonds are known to form. The splitting between the C and O core level BE's, as compared with the gas phase values, suggests that this perturbation leads to small BE shifts of the oxygen level. Deconvolution of the O and C(KVV) Auger transitions in the condensed layer could confirm this point.

As the surface temperature is increased, the condensed multilayers desorb beginning at ~170 K leaving a layer of an oxygen and carbon containing moiety with shifted core level BE's and pronounced changes in the valence region compared to gas phase, chemisorbed, and condensed CH_3OH. This species is identified as surface methoxide on the basis of theoretical predictions and interpretation of changes in the spectral features. Whether the methoxide layer is formed, i.e., cleavage of the hydroxyl hydrogen, before desorption of the condensed multilayers awaits further experimentation as does the fate of the hydroxyl hydrogen. The methoxide complex can also be formed by CH_3OH absorption at temperatures greater than 170 K.

The methoxide complex is stable to ~500 K but further temperature increases lead to a decomposition of the complex concurrent with efficient oxidation of the substrate and the evolution of CH_4. The O(2p) resonance after this decomposition is indistinguishable from that obtained by oxidation of the Al substrate with O_2 though some residual uncharacterized

carbon remains on the surface.

As compared to transition metals, the absence of d-electrons in Al drastically alters the adsorption behavior and temperature stability of CH_3OH. Additional studies on metals such as Mg and Ca would further our understanding of the role of d-electrons in the stability of methoxide-like complexes. Other alcohols should also be examined on Al to determine if alkoxides are stable in general. Metals with filled d-bands are, in general, not as easily oxidized as Al. Providing a methoxide complex could be stabilized at higher temperature on such a surface, some very interesting chemistry could occur after co-adsorption of another species.

References

1. Chem. Week, June 27, 1979, p. 29.
2. R. T. Johnson and R. K. Riley, "Evaluation of Methyl Alcohol as a Vehicle Fuel Extender", University of Missouri, August, 1975. Available from Ref. 5, PB 251-108.
3. S. E. Voltz and J. J. Wise, Mobil Research and Development Corp., November 1976. Available from Ref. 5, FE 1773-25.
4. R. F. Pefley, L. H. Browning, W. E. Likos, M. C. McCormack and B. Pullman, "Characterization and Research Investigation of Methanol and Methyl Fuels", The University of Santa Clara, August 1977. Available from Ref. 5, PB 271-889.
5. National Technical Information Service, U.S. Department of Commerce, 5285 Port Royal Road, Springfield, VA 22151.
6. M. B. Robin and N. A. Kuebler, J. Electron Spectrosc. Related Phenomena, 1 (1972/73) 13.
7. G. W. Rubloff and J. F. Demuth, J. Vacuum Sci. Technol. 14 (1977) 419.
8. J. E. Demuth and H. Ibach, Chem. Phys. Letters, 60 (1979) 395.
9. W. F. Egelhoff, J. W. Linnett and D. L. Perry, Faraday Disc. Chem. Soc., 60, (1976) 127.
10. W. F. Egelhoff, Jr., D. L. Perry, and J. W. Linnett, J. Electron Spectrosc. Related Phenomena, 5 (1974) 339.
11. [illegible]n B. Fisher, Theodore E. Madey, Bernard J. Waclawski and J. T. Yates, Jr., in: Proc. 7th Intern. Vac. Congr. & 3rd Intern. Conf. Solid Surfaces, (Vienna, 1977) 1071.
12. M. Bowker and R. J. Madix, Presented at the Pacific Conference on Chemistry and Spectroscopy, (Pasadena, California, 1979).

13. H. Luth, G. W. Rubloff and W. D. Grobman, Surface Sci., 63 (1977) 325.
14. K. Y. Yu, J. C. McMenamin and W. E. Spicer, J. Vacuum Sci. Technol., 12 (1975) 286.
15. G. W. Rubloff, H. Luth and W. D. Grobman, Chem. Phys. Letters, 39 (1976) 493.
16. G. D. Parks and M. J. Dreiling, private communication.
17. J. W. Rogers, Jr. and J. M. White, J. Vacuum Sci. Technol., 16 (1979) 485.
18. J. W. Rogers, Jr., Ph.D. Dissertation, University of Texas at Austin, December 1979.
19. J. W. Rogers, Jr., R. L. Hance and J. M. White, to be published.
20. CH_3OH could be dissociated with both oxygen and carbon containing fragments remaining on the surface but the UPS results presented below rule out this possibility.
21. It is assumed that the Al(2s) attenuation length is comparable in the condensed layer to that in Al metal. See D. Briggs, Ed., "Handbook of X-ray and Ultraviolet Photoelectron Spectroscopy" (Heyden, London, 1977) p. 222 for a discussion of mean free paths in molecular and metallic solids.
22. Calculated from van der Waals radii. "Handbook of Chemistry and Physics", 50th Ed., R. C. Weast, Ed., (CRC Press, Cleveland, 1969) p. F157.
23. See Ref. 21, page 137.
24a. G. B. Fisher, N. E. Erikson, T. E. Madey and J. T. Yates, Jr., Surface Sci. 65 (1977) 210.
24b. P. R. Antoniewicz, private communication.

25. M. O. Krause and J. H. Oliver, J. Phys. Chem. Ref. Data, 8 (1979) 329.

26. K. Siegbahn, C. Norlding, G. Johannson, J. Hedman, P. F. Heden, K. Hamrin, U. Gelius, T. Bergmark, L. O. Werme, R. Manne and Y. Baer, "ESCA Applied to Free Molecules", (North-Holland, New York, 1969) p. 22. Siegbahn's value of 1.5 eV was convoluted with our instrument resolution (1.6 eV) and the Mg (Kα) natural line width (0.8 eV) before comparison with the present data. They did not report a C(1s) peak width.

27. Our thanks to Mike Lattman for the gas phase CH_3OH spectrum.

28. Reprinted with permission: W. L. Jorgensen and L. Salem, "The Organic Chemist's Book of Orbitals", (Academic Press, New York, 1973) p. 105.

29. J. H. R. Eland, "Photoelectron Spectroscopy", (Butterworths, London, 1974) p. 22, 23. Eland misinterpreted the origin of the third band but the description presented here is currently thought to be correct.

30. G. W. Rubloff and J. E. Demuth, J. Vacuum Sci. Technol., 14 (1977) 419.

31. R. M. Eastment and C. H. B. Mee, J. Physics F: Metal Physics, 3 (1973) 1738.

32. Previously we aligned spectra via the $(4a')^{-1}$ transition. Due to its core-like nature and differences between relaxation phenomena in core and valence orbitals [33,34] as well as the fact that some hydrocarbon systems exhibit unusual relaxation shifts in this C(2s) derived transition [35] we decided that the $(1a'')^{-1}/(6a')^{-1}$ transition was more appropriate for alignment of the CH_3OH valence band.

33. B. Feuerbacher, B. Fitton and R. F. Willis, Eds., "Photoemission and the Electronic Properties of Surfaces", (Wiley Interscience, New York, 1978) p. 359.

34. J. E. Demuth, Phys. Rev. Letters, 40 (1978) 409.

35. G. W. Rubloff, W. D. Grobman and H. Luth, Phys. Rev. B, 14 (1976) 1450.

36. H. Luth, G. W. Rubloff and W. D. Grobman, Surface Sci., 63 (1977) 325.

37. H. D. Hagstrum, Surface Sci., 54 (1976) 197.

38. J. E. Demuth, Phys. Rev. Letters, 40 (1978) 409.

39. M. J. Campbell, J. Liesegang, J. D. Riley, R. C. G. Leckey, J. G. Jenkin, and R. T. Poole, J. Electron Spectrosc. Related Phenomena, 15 (1979) 83.

40. L. Pauling, "The Nature of the Chemical Bond", (Cornell Univ. Press Ithaca, 1939) p. 284.

41. P. A. Redhead, Vacuum, 12 (1962) 203.

42. P. H. Holloway, T. E. Madey, C. T. Campbell, R. R. Rye and J. E. Houston, Surface Sci., 88 (1979) 121.

43. D. Edwards, Jr., J. Vacuum Sci. Technol., 16 (1979) 695.

44. Demuth and Ibach recently confirmed this species as methoxide using high resolution electron energy loss spectroscopy [8].

45. D. C. Bradley, "Advances in Inorganic Chemistry and Radiochemistry" Vol. 15, (Academic Press, New York, 1972) p. 259-323.

46. El-Ahmadi, I. Heiba and P. S. Landis, New York, J. Catalysis, 3 (1964) 471.

47. R. C. Baetzold and G. A. Somorjai, J. Catalysis, 45 (1976) 94.

Figure Captions

Figure 1. O(1s) and C(1s) XPS spectra for various exposures of CH_3OH on Al at 110K. Mg K_α x-rays of energy 1253.6 eV were used.

Figure 2. O(1s) peak area as a function of CH_3OH exposure at 120K.

Figure 3. (a) Al(2s) peak area versus relative CH_3OH coverage (from Fig.2) for CH_3OH on polycrystalline Al at 120K. Dashed line is a smooth curve through all the data points. See text for monolayer attenuation calculation.

(b) Binding energies for O(1s), O, and C(1s), Δ, as a function of CH_3OH coverage at 120K.

(c) Peak widths at half maximum for O(1s), O, and C(1s), Δ, peaks as a function of CH_3OH coverage.

Figure 4. Gas phase UPS spectrum of CH_3OH [27] and valence level molecular orbital representations for methanol, reproduced with permission from reference [28].

Figure 5. He II UPS spectra for CH_3OH adsorption on clean Al under various conditons: a) clean Al at 300K, b) low coverage of methoxide at 300K, c) saturation coverage of methoxide at 300K, d) chemisorbed methanol at 110K and e) multilayer methanol at 110K. Gas phase ionization potentials [6], for comparison with spectrum e only and referenced to E_{F}, are shown at the top. The work function changes are as follows: b)$\Delta\phi$ = -0.3 eV, c) -0.9 eV, d) -1.0 eV and e) -1.3 eV.

Figure 6. Behavior of O(1s), C(1s) and Al(2s) peak areas for CH_3OH condensed on Al at 120K and warmed to various temperatures. Arrow marks position of thermal desorption maximum monitored by mass spectrometry.

Figure 7. O(1s) and C(1s) peaks for adsorption of CH_3OH and O_2 under various conditions: a) and d) 75L CH_3OH at 300K, b) and e) 3L CH_3OH at 110K, c) 3L O_2 at 110K and f) 30L CH_3OH at 110K plus heat to 300K.

Figure 8. He II UPS spectra of (a) saturation coverage of surface methoxide at 300K and (b) oxide remaining after heating saturated methoxide from 300 to 573K.

SS 8001

TABLE 1

Binding Energies (eV) of CH_3OH/Al (T = 110-500 K)

Orbital	Gas [a]	Chemisorbed	Condensed	Methoxide [d]
2a"	8.06	6.7	6.6 [b]	7.4
7a'	9.72	8.0	8.6 [b]	
1a"/6a'	12.53	11.0	11.0 [b]	
5a'	14.72	13.4	13.4 [b]	11.2
4a'	19.75	18.4	18.7 [b]	18.4
C(1s)	289.4	286.7	287.2 [c]	287.1
O(1s)	536.0	532.3	533.3 [c]	532.7

[a] Referenced to E_F by subtracting $(\Phi_{Al} + \Delta\Phi_{sat})$ = 2.9 eV from the gas phase IP's. The valence orbital data is from ref. 6 and the core orbital data from ref. 26.

[b] Shifted 0.6 eV to lower BE to align the 1a" orbitals.

[c] Determined from Fig. 3b ; see text.

[d] Condensed CH_3OH + heat to 190 K or adsorption at 150-473K.

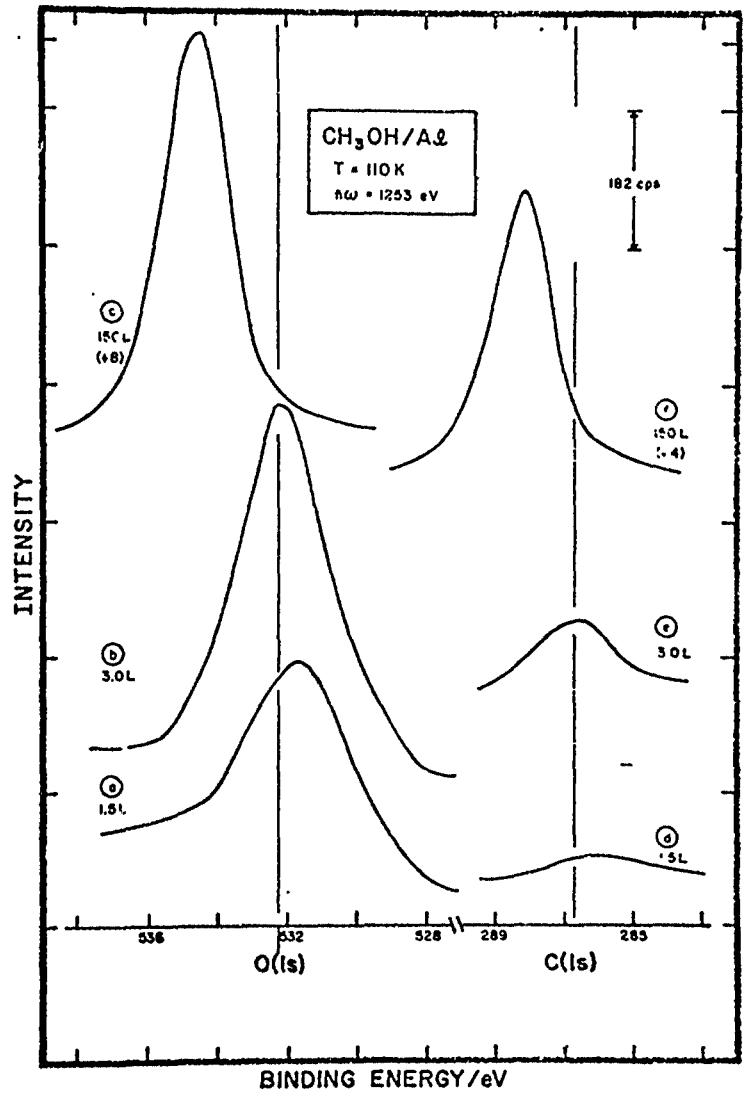

Rogers et.al. Fig.1

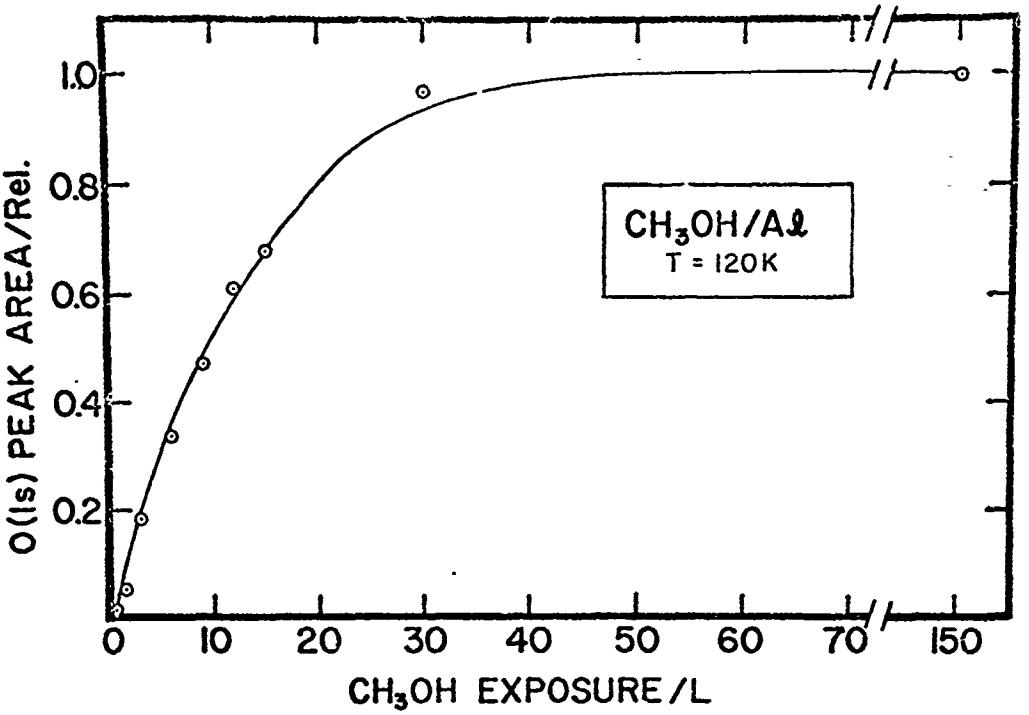

28

Rogers et al. Fig. 2.

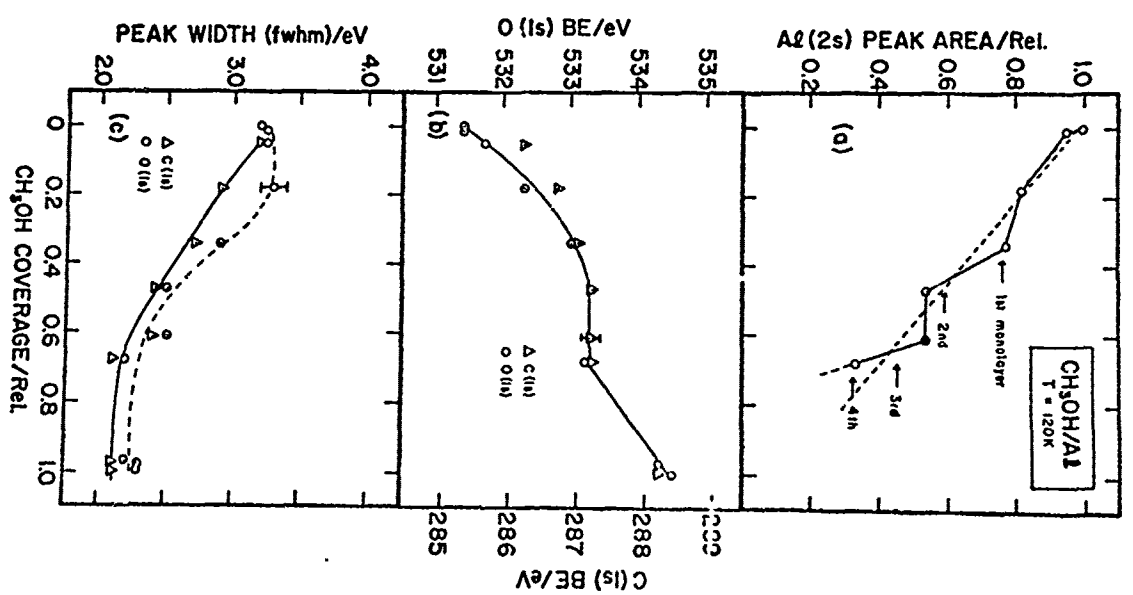

Rogers et al. Fig. 3

29

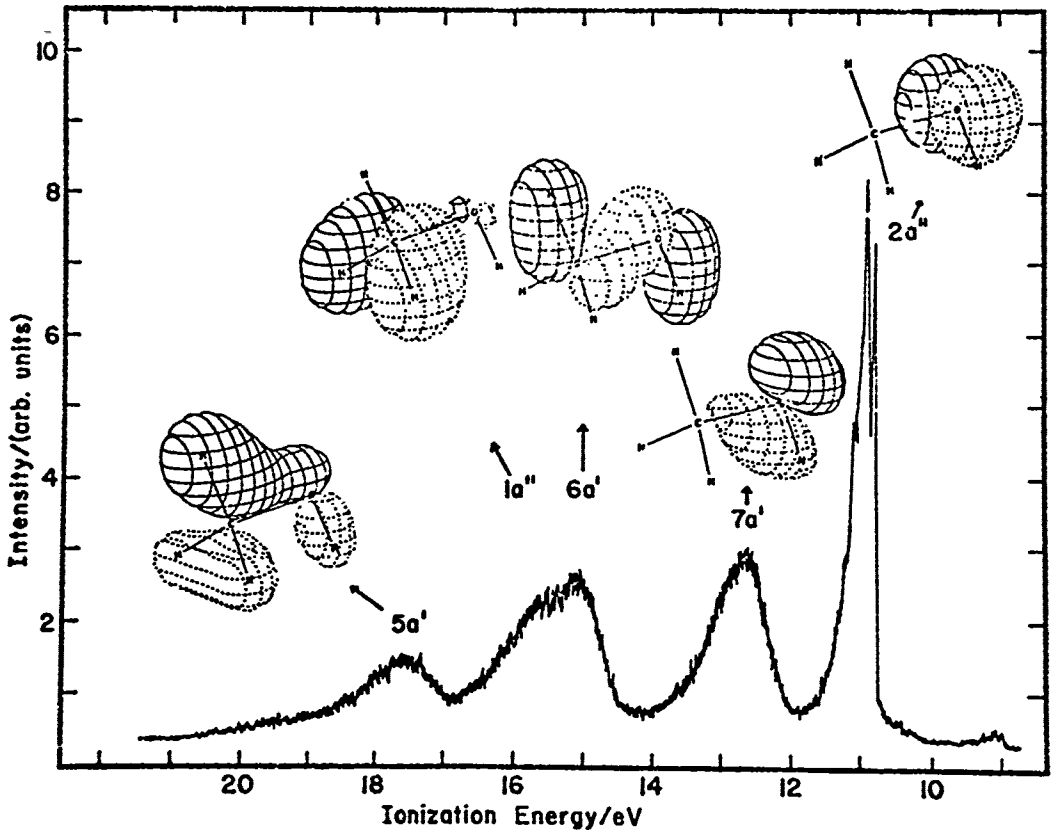

Donon et al 7:4.

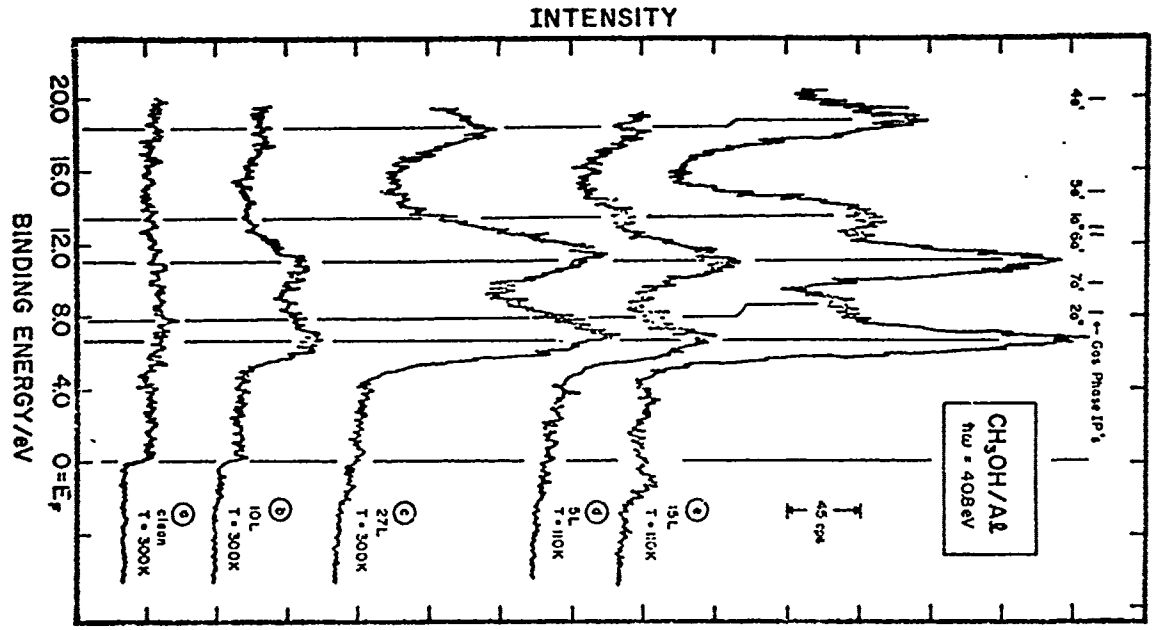

Rogers et al. Fig. 5

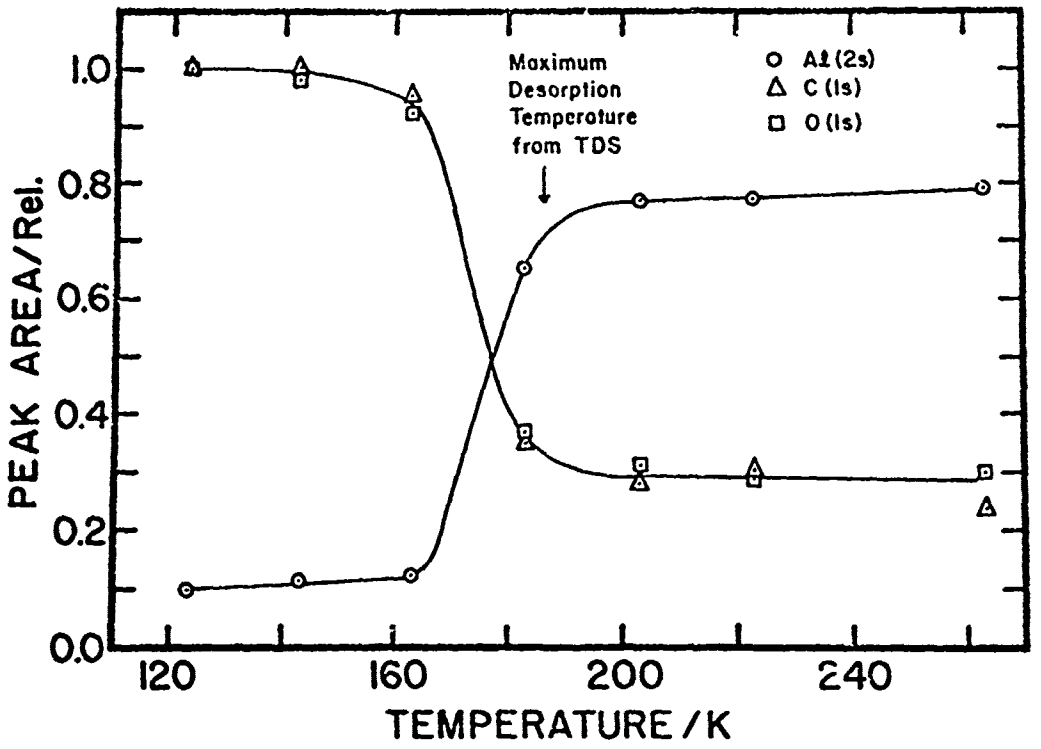

32

Rosen et. al. Fig. 6

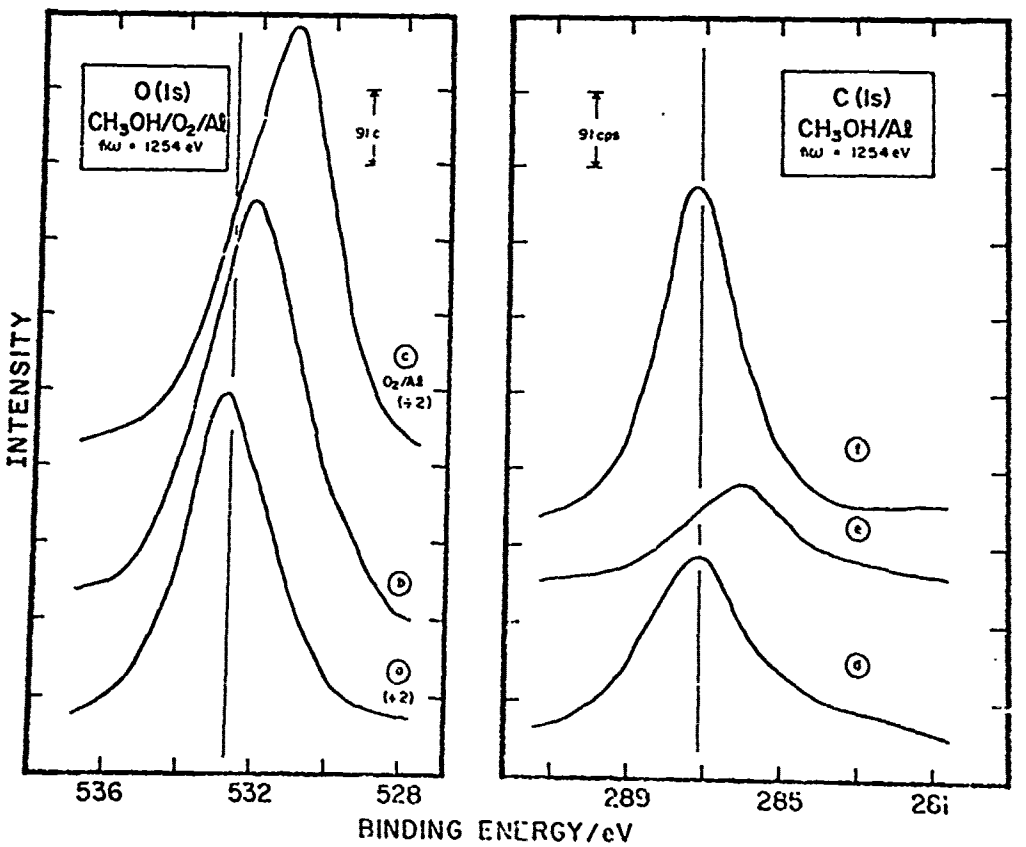

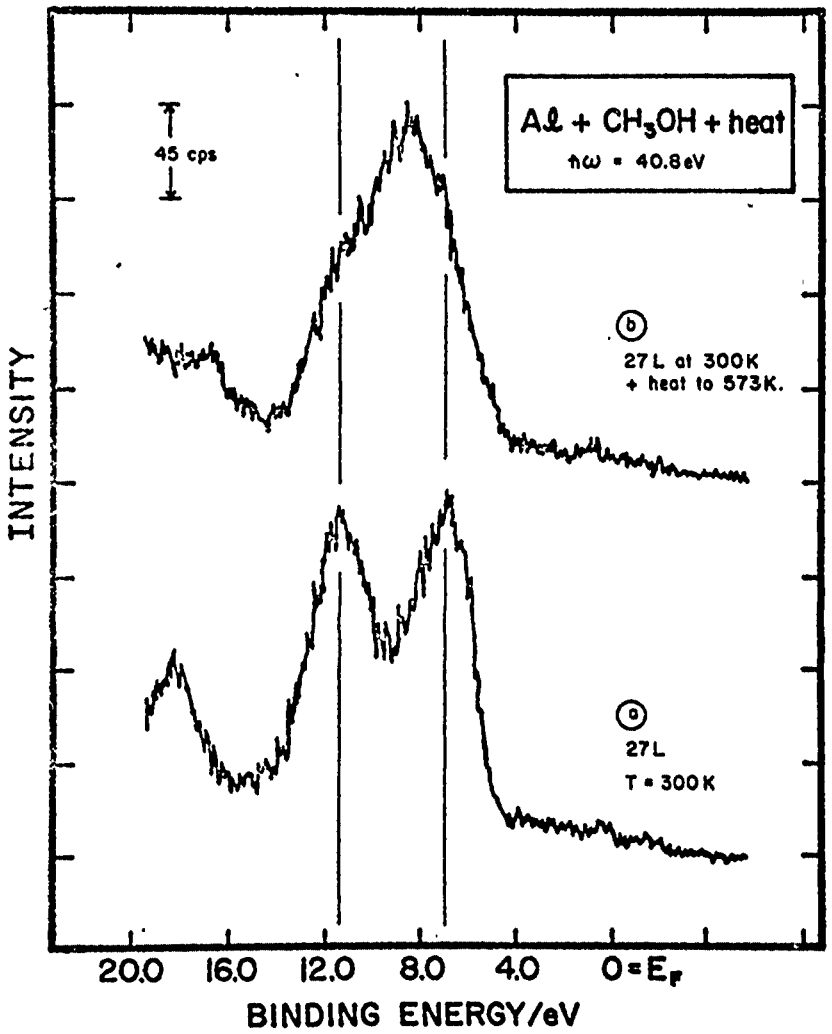

Rogers et al. Fig. 8.